Available online at www.sciencedirect.com
ScienceDirect
Journal of the Chinese Institute of Chemical Engineers 38 (2007) 71–84
JOURNAL OF THE CHINESE INSTITUTE OF CHEMICAL ENGINEERS
www.elsevier.com/locate/jcice

Equilibrium and kinetics of heavy metal ion exchange

I-Hsien Lee [1], Yu-Chung Kuan [2], Jia-Ming Chern [3,*]

Department of Chemical Engineering, Tatung University, Taipei 10452, Taiwan

Received 15 August 2006; accepted 20 November 2006

Abstract

Ion exchange has a great potential to remove heavy metals from industrial wastewaters or heavy metal-containing sludge. In order to design and operate heavy metal removal processes, the equilibrium relationship between ions and resin must be known a prior. A series of ion-exchange equilibrium tests of Cu^{2+}/H^+, Zn^{2+}/H^+, and Cd^{2+}/H^+ systems using Amberlite IR-120 were performed. The equilibrium data were analyzed by the Langmuir isotherm, Freundlich isotherm, and selectivity coefficient approaches. The thermodynamic parameters such as Gibbs free energy change, enthalpy change, and entropy change were calculated. By comparison of the selectivity coefficients, the affinity sequence to IR-120 is $Cu^{2+} > Zn^{2+} > Cd^{2+} > H^+$. Moreover, in order to understand the heavy metal extraction kinetics in the presence of Amberlite IR-120, the ion-exchange kinetics was also studied. The ion-exchange kinetic data were regressed by the pseudo first-order, second-order models, and a reversible reaction model. The activation energies calculated from the rate coefficients at different temperatures are 15.41, 7.04, and 17.01 kJ/mol for copper, zinc, and cadmium, respectively. Although the pseudo first- and second-order models are easier to use for data analysis, the resultant model parameters depend on operating conditions. The reversible reaction model is capable to predict the effects of resin to solution ratio, initial heavy metal concentration, and temperature on the ion-exchange kinetic curves.
© 2007 Taiwan Institute of Chemical Engineers. Published by Elsevier B.V. All rights reserved.

Keywords: Heavy metal; Ion exchange; Equilibrium; Kinetics; Thermodynamics

1. Introduction

Nowadays, water plays an important role in human beings, natural environment, and social development, but the subsequences of water use are municipal wastewaters and industrial wastewaters. Therefore, how to treat wastewaters and make them reusable is not only an important task but also an urgent problem to be solved. Industrial wastewaters from many factories contain heavy metals such as copper, zinc, cadmium, lead, nickel, and chromium that will damage environment. The most popular method to treat heavy metal-containing wastewaters is chemical precipitation that uses alkaline to raise the solution pH to allow the formation of heavy metal hydroxide precipitate followed by filtration or other solid/liquid separation processes. Although the chemical precipitation method is quite effective for heavy metal removal, the resultant heavy metal sludge is classified as a hazardous solid waste and needs to be adequately treated. Sometimes, treating heavy metal sludge is more difficult than treating heavy metal-containing wastewaters. Therefore, other methods such as electrodialysis (Mohammadi *et al.*, 2004, 2005; Schlichter *et al.*, 2004), reverse osmosis (Kryvoruchko *et al.*, 2004; Ujang and Anderson, 1998), biosorption including some economic bio-adsorbent (Aksu and Dönmez, 2001; Bhattacharyya and Sharma, 2004; Evans *et al.*, 2002; Kapoor and Viraraghavan, 1998; Sağ and Kutsal, 1995; Tarley and Arruda, 2004), adsorption (Choi *et al.*, 2006; Lyubchik *et al.*, 2004; Park and Kim, 2005; Suh and Kim, 2000; Yu *et al.*, 2000), and ion exchange process are developed to remove heavy metals from industrial wastewaters.

Among the heavy metal removal processes, ion exchange process is very effective to remove various heavy metals and can be easily recovered and reused by regeneration operation. Ion-exchange resins are a variety of different types of exchange materials, which are distinguished into natural or synthetic resin. Furthermore, it can be as well categorized on the basis of functional groups such as cationic exchange resins, anion exchange resins, and chelating exchange resins (Dorfner, 1991). Depending on the functional groups, ion-exchange resin

* Corresponding author. Tel.: +886 2 27002737x23; fax: +886 2 27087819.
E-mail address: jmchern@ttu.edu.tw (J.-M. Chern).
[1] 李逸先
[2] 管郁中
[3] 陳嘉明

0368-1653/$ – see front matter © 2007 Taiwan Institute of Chemical Engineers. Published by Elsevier B.V. All rights reserved.
doi:10.1016/j.jcice.2006.11.001

Nomenclature

C	total metal concentration in the solution phase
C_0	initial heavy metal concentration in solution phase
C_e	heavy metal concentration in solution phase at equilibrium
C_H	hydrogen ion concentration in the solution phase
C_M	metal ion concentration in the solution phase
F_c	dimensionless factor defined in Eq. (18)
H^+	hydrogen ion in solution phase
K	Langmuir isotherm parameter defined in Eq. (2)
K_{MH}	selectivity coefficient defined in Eq. (4)
K'_{MH}	modified selectivity coefficient defined in Eq. (5)
k_1	rate constant of pseudo first-order kinetic model defined in Eq. (9)
k_2	rate constant of pseudo second-order kinetic model defined in Eq. (11)
k_a	forward rate constant of reversible reaction model defined in Eq. (13)
k_b	backward rate constant of reversible reaction model defined in Eq. (13)
k_f	Freundlich isotherm constants defined in Eq. (3)
M^{2+}	divalent metal ions in the solution phase
N	Langmuir isotherm parameter defined in Eq. (2)
n	Freundlich isotherm parameter defined in Eq. (3)
q_c	metal concentration capacity in the resin phase
q_e	metal concentration in the resin phase at equilibrium
q_H	hydrogen ion concentration in the resin phase
q_M	metal concentration in the resin phase at reaction time t
R	gas constant
R^2	R-square value
RH	ion-exchange resin in hydrogen form
R_2M	exchanged metal onto ion-exchange resin
T	temperature
t	reaction time
V	volume of the solution
W_R	dry weight of the ion-exchange resin
x_H	hydrogen equivalence fraction in the solution phase
x_M	metal equivalence fraction in the solution phase
y_H	hydrogen equivalence fraction in the resin phase
y_M	metal equivalence fraction in the resin phase

Greek symbols

ΔG	Gibbs free energy change defined in Eq. (7)
ΔH	enthalpy change defined in Eq. (7)
ΔS	entropy change defined in Eq. (7)

can deal properly with several heavy metals such as copper, nickel, cobalt, cadmium, zinc, and aluminum (Ersoz *et al.*, 1995; Fernández *et al.*, 2005; Kiefer and Höll, 2001; Kilislioglu and Bilgin, 2003).

In addition to removing heavy metals from industrial wastewater, ion-exchange resin can facilitate heavy metal extraction from sludge by shifting the thermodynamic equilibrium of $M(OH)_{2(s)} \leftrightarrows M^{2+} + 2OH^-$. The sludge solid and the slightly dissolved metal ions in the solution can be disturbed in the presence of cationic ion-exchange resin according to the Le Chatelier principle. The hydrogen ions released from the cationic ion-exchange resin will neutralize the hydroxide ions so that the equilibrium will shift until all the metal ions are leached into solution and adsorbed onto the ion-exchange resin. An experimental study of heavy metal sludge extraction was conducted by the authors (Lee *et al.*, 2006), using both Amberlite IRC-718 and Amberlite IR-120. The stronger cationic exchange resin, Amberlite IR-120, was found to favor a lower heavy metal residue in the sludge. Therefore, another study aimed at understanding the heavy metal extraction kinetics in the presence of Amberlite IR-120 is being conducted.

Similar to adsorption process, equilibrium and kinetics for a chosen ion exchange resin under various experimental conditions are quite important and always studied at the beginning of the research. There are many approaches that can be used to describe the ion-exchange equilibrium at present. However, the ion-exchange kinetics based on the Nernst–Planck equation with true diffusion limitation is rather complex; some empirical or simplified rate equations, therefore, are used (Chiron *et al.*, 2003; Juang *et al.*, 2006; Lin and Juang, 2005; Ribeiro and Ribeiro, 2005; Sekar *et al.*, 2004). Although these simplified rate equations are not accurate and can be accommodated to every experimental conditions, they are still readily and indispensable for the theoretical analysis of complex phenomena such as ion exchange in columns and system with more than two counter-ion species (Dranoff and Lapidus, 1958, 1961; Helfferich, 1962). This study therefore aims at determining suitable ion-exchange equilibrium and kinetic models of Cu^{2+}/H^+, Zn^{2+}/H^+, and Cd^{2+}/H^+ systems for Amberlite IR-120. Such ion-exchange equilibrium and kinetic models will be incorporated in the future kinetic model for heavy metal extraction from sludge in the presence of Amberlite IR-120.

2. Materials and methods

2.1. Cationic exchange resin and reagents

Amberlite IR-120 (Rohm Haas Corp., USA), a strong cationic ion-exchange resin with effective particle size from 0.43 to 0.55 mm and 44 to 48% moisture content, was used in this study. Before experiments the resin was acid-conditioned with 1N HCl (Yakuri Pure Chemicals Corp., Japan) several times to remove impurity from the resin and to convert the exchange sites to the desired H^+ form. Then part of the conditioned ion-exchange resin was dried at 333 K for physical properties determination. The heavy metal solutions were prepared by copper nitrate, zinc nitrate, and cadmium nitrate with purity greater than 95.0% (Wako Pure Chemicals Corp.,

Japan) and deionized water. About 3 g of the conditioned resin was placed in a glass column and a known amount of standard 0.1N sodium hydroxide solution was fed to the column at a low flow rate in order to determine the ion-exchange capacity of the resin.

2.2. Ion-exchange equilibrium experiments

In order to obtain the ion-exchange equilibria of Cu^{2+}/H^+, Zn^{2+}/H^+, and Cd^{2+}/H^+ systems at desired temperatures 298, 328, and 358 K, different amounts of the conditioned resin in H-form were put into several PE bottles, each of them filled with 500 mL heavy metal solution with desired concentrations. The bottles were shaken for 24 h in a temperature-controlled shaker (Hotech Inc., Corp., Model 706) to reach ion-exchange equilibrium. At the end of equilibrium, the resin was separated from the solution by filtration and the equilibrium metal concentration in the solution was determined by the Atomic Absorption Spectrophotometer (Varian, Model 3000). The metal concentration exchanged onto the resin was calculated by mass balance relation as following equation:

$$q = \frac{(C_0 - C)V}{W_R}, \tag{1}$$

where C_0 and C are the initial and final metal concentrations in the solution phase, respectively; q is the metal concentration in the resin phase; V is the solution volume; and W_R is the dry weight of the resin used in the test. In order to measure the metal concentration in the solution phase, the calibration relationship between AAS and each heavy metal concentration was determined before experiment. All R-square values of calibration data fitted by linear regression method are greater than 0.999 for copper, zinc, and cadmium system. The errors of measurement for experimental samples are very small and acceptable.

2.3. Ion-exchange kinetic experiments

The ion-exchange kinetic experiments were carried out in a 2-L jacketed batch reactor in order to control the reaction temperature at desired level. Our preliminary tests using varying agitation speeds showed that the 350 rpm was high enough to well suspend the ion exchange resin, to eliminate the external mass-transfer resistance. Therefore, 350 rpm was used for all the experimental test runs. During the kinetic experiments, solution samples were taken from the reactor at desired time intervals to determine the heavy metal concentrations by atomic absorption spectrophotometer. The metal concentration exchanged onto the resin was also calculated by mass balance relation shown in Eq. (1). The ion-exchange kinetics of copper, zinc, and cadmium was measured at varying resin amounts, initial metal concentrations, and temperatures. In this study, the solution volume for each test was 1 L. Other experimental conditions of all ion-exchange kinetic runs were listed in Table 1.

3. Results and discussion

3.1. Ion-exchange equilibria

Ion-exchange equilibria of copper, zinc, and cadmium were first measured at 298 K, and the experimental data were analyzed by the Langmuir and Freundlich isotherms:

$$q_e = \frac{KNC_e}{1 + KC_e}, \tag{2}$$

$$q_e = k_f C_e^n \tag{3}$$

where q_e is the metal concentration in the resin phase at equilibrium and C_e is the metal concentration in the solution phase at equilibrium; K, N, k_f, and n represent the Langmuir and Freundlich isotherm constants, respectively. Both of these two equations can be rearranged to a linear relationship; the plots of C_e/q_e versus C_e and $\log(q_e)$ versus $\log(C_e)$ should be straight lines from which the coefficients can be determined by the slopes and intercepts.

The adsorption isotherm coefficients obtained from the slopes and intercepts of the linear plots are listed in Table 2. As shown by the R^2 in Table 2, the Langmuir adsorption isotherm provides a better fit to the experimental data of copper, zinc, and cadmium isotherm than the Freundlich approach. There are no significant relations for the parameters and the temperature. Comparing these parameters, the resin affinity sequence seems to be $Cu^{2+} > Zn^{2+} \approx Cd^{2+}$.

Although the Freundlich isotherm approach is widely used to interpret adsorption and ion-exchange equilibrium data, the

Table 1
Experimental conditions of ion-exchange kinetic tests

Run no.	Metal	Initial metal concentration (meq/L)	Reaction temperature (K)	Ion-exchange resin weight (g)
1	Cu^{2+}	4.7	298	2.0
2	Cu^{2+}	4.7	298	3.0
3	Cu^{2+}	4.7	298	4.0
4	Cu^{2+}	4.7	298	5.0
5	Cu^{2+}	2.6	298	2.0
6	Cu^{2+}	1.4	298	2.0
7	Cu^{2+}	0.4	298	2.0
8	Zn^{2+}	4.7	298	2.0
9	Zn^{2+}	3.3	298	2.0
10	Zn^{2+}	1.8	298	2.0
11	Zn^{2+}	0.6	298	2.0
12	Cd^{2+}	3.1	298	2.0
13	Cd^{2+}	2.3	298	2.0
14	Cd^{2+}	1.5	298	2.0
15	Cd^{2+}	0.6	298	2.0
16	Cu^{2+}	4.7	318	2.0
17	Cu^{2+}	4.7	338	2.0
18	Cu^{2+}	4.7	358	2.0
19	Zn^{2+}	4.5	318	2.0
20	Zn^{2+}	4.4	338	2.0
21	Zn^{2+}	4.4	358	2.0
22	Cd^{2+}	3.1	318	2.0
23	Cd^{2+}	3.1	338	2.0
24	Cd^{2+}	3.1	358	2.0

Table 2
Ion-exchange equilibrium parameters of Langmuir and Freundlich isotherms at different temperatures

Metal	T (K)	K (L/meq)	N (meq/g)	R^2
Langmuir isotherm				
Cu^{2+}	298	21.147	1.652	0.9971
	328	63.429	1.504	0.9840
	358	122.964	1.559	0.9877
Zn^{2+}	298	23.803	1.341	0.9929
	328	61.813	1.117	0.9039
	358	147.914	1.185	0.9795
Cd^{2+}	298	34.081	1.350	0.9617
	328	16.331	1.135	0.9756
	358	237.573	1.169	0.9367
Metal	T (K)	k_f	n	R^2
Freundlich isotherm				
Cu^{2+}	298	1.627	0.206	0.9513
	328	1.450	0.116	0.9692
	358	1.533	0.108	0.9623
Zn^{2+}	298	1.293	0.169	0.9585
	328	1.128	0.129	0.9252
	358	1.214	0.117	0.9658
Cd^{2+}	298	1.366	0.172	0.9037
	328	1.206	0.128	0.9384
	358	1.207	0.101	0.8925

equation is empirical in nature. For ions with the same valence, ion-exchange equilibrium described by the constant separation factor is of the same form of the Langmuir isotherm. But for ions with different valences, such as heavy metal and hydrogen ions, the ion-exchange equilibrium should be better described by the selectivity coefficient defined as (Helfferich, 1962):

$$K_{MH} = \left(\frac{q_M}{C_M}\right)\left(\frac{C_H}{q_H}\right)^2, \tag{4}$$

where K_{MH} is the selectivity coefficient based on concentration for heavy metal M and hydrogen H; q_i and C_i are the species concentrations in the resin and solution phases, respectively. The species concentrations can be expressed in terms of the equivalence fraction. Therefore, Eq. (4) can be rewritten as:

$$K'_{MH} = K_{MH}\frac{q_c}{C} = \left(\frac{y_M}{x_M}\right)\left(\frac{x_H}{y_H}\right)^2, \tag{5}$$

where K'_{MH} is the selectivity coefficient based on equivalence fraction; C and q_c are the total cation concentrations in the solution and resin phases, respectively. Since the summations of the equivalence fractions of the heavy metal and hydrogen in the solution and resin phases both equal unity, the heavy metal equivalence fraction in the resin phase can be expressed in terms of that in the solution phase:

$$y_M = 1 - \frac{-1 + \sqrt{1 + ((4K'_{MH}x_M)/(1-x_M)^2)}}{((2K'_{MH}x_M)/(1-x_M)^2)}. \tag{6}$$

The selectivity coefficient based on equivalence fraction can be obtained from fitting the experimental ion-exchange isotherm data to Eq. (6) and then it can be used to calculate the selectivity coefficient based on concentration. It is important to note that selectivity coefficient based on concentration K_{MH} is a true constant, but the selectivity coefficient based on equivalence fraction K'_{MH} depends on the total solution concentration and the resin exchange capacity.

Table 3 summarizes the selectivity coefficients from a series of batch experiments at different reaction temperatures for copper, zinc, and cadmium. Compared with the Langmuir approach that has two adjustable parameters, there is only one parameter used in the selectivity coefficient approach. The correlation coefficients R^2 values shown in Table 3 are not as high as those of the Langmuir approach. However, the R^2 values listed in Table 3 suggest the single-parameter model provides a close enough fit to the experimental data as also shown by Fig. 1. The fitted isotherms at different temperatures using selectivity coefficients were plotted in Fig. 1 in order to compare the effect of temperature. All the figures show that the equilibrium isotherms are of favorable types. This suggests that all the heavy metals have affinity greater than the hydrogen ion. Therefore, IR-120 in H-form should be effective to remove the three heavy metals from wastewaters. As shown by the selectivity coefficients in Table 3, the affinity sequence in this system is: $Cu^{2+} > Zn^{2+} \approx Cd^{2+} > H^+$.

The same heavy metal/hydrogen ion exchange systems using IR-120 at different temperatures were also studied by Valverde *et al*. (2002). Unlike this study, Valverde *et al*. used the Wilson and Pitzer equations to calculate the activity coefficients in the resin and liquid phases, respectively. Their

Table 3
Selectivity coefficients of heavy metal ion exchange at different temperatures

Metal	Total cation concentration (meq/L)	Parameter	Selectivity coefficient (K_{MH}) at varying temperatures				
			This study			Valverde (2002)	
			298 K	328 K	358 K	283 K	303 K
Cu^{2+}	1.29 ± 0.25	K_{MH}	40.43	97.32	174.82	50.41	67.79
		R^2	0.9794	0.9731	0.9472	NA	NA
Zn^{2+}	1.04 ± 0.08	K_{MH}	37.48	61.69	109.66	46.93	76.74
		R^2	0.9777	0.9186	0.9838	NA	NA
Cd^{2+}	0.83 ± 0.06	K_{MH}	37.44	68.77	100.07	31.02	38.01
		R^2	0.9332	0.9731	0.9472	NA	NA

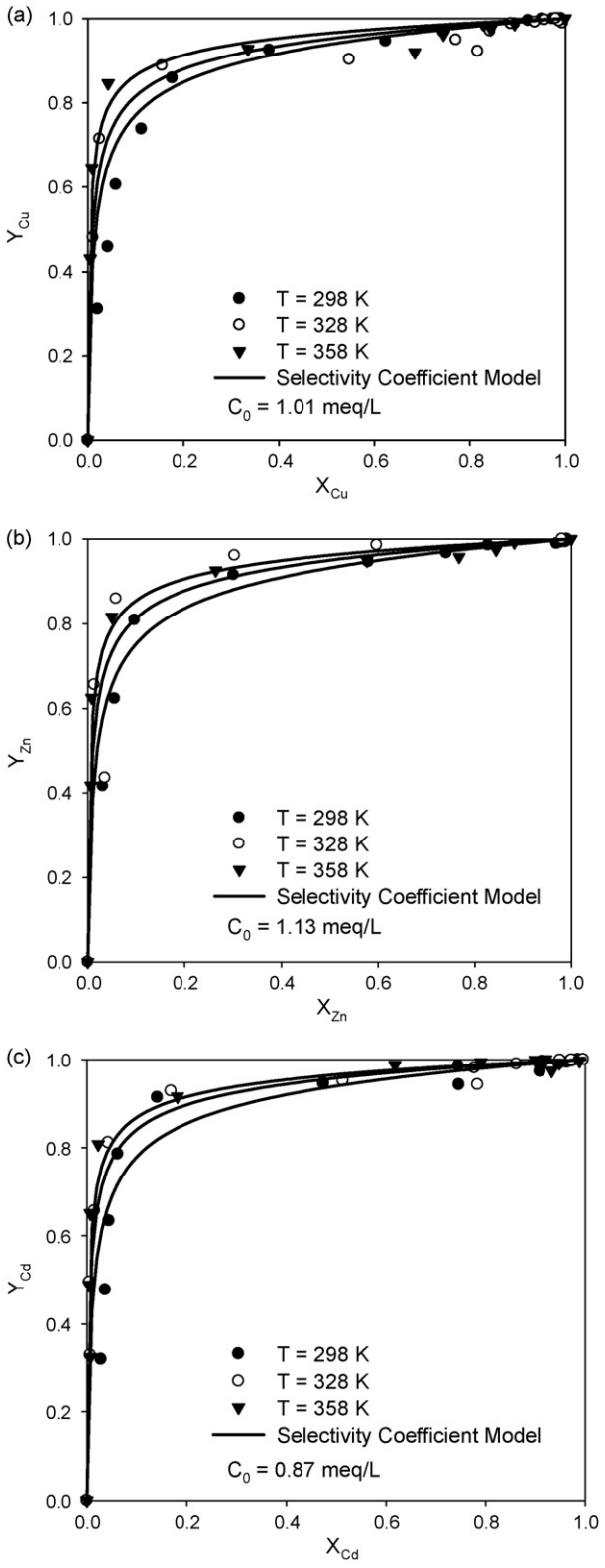

Fig. 1. Experimental and predicted ion-exchange equilibria of (a) Cu^{2+}/H^+, (b) Zn^{2+}/H^+, and (c) Cd^{2+}/H^+ systems at different temperatures.

equilibrium constants based on activity at 283 K and 303 K are also listed in Table 3. The true equilibrium constants calculated by Valverde *et al*. are greater than those obtained in this study. According to the equilibrium constants of Valverde *et al*., the ion-exchange resin exhibits different orders of selectivity at 283 K and 303 K, being $Cu^{2+} > Zn^{2+} > Cd^{2+}$ at 283 K and $Zn^{2+} > Cu^{2+} > Cd^{2+}$ at 303 K.

3.2. Thermodynamic parameters of ion exchange

The selectivity coefficients at 298, 328, and 358 K for copper, zinc, and cadmium shown in Table 3 suggest that these coefficients are related to the reaction temperature. For ion-exchange process, the following thermodynamic relationship is applicable:

$$\Delta G = \Delta H - T\Delta S, \tag{7}$$

where T is the reaction temperature; ΔG is the Gibbs free energy change; ΔS is the entropy change; and ΔH is the enthalpy of ion-exchange process. In order to obtain the relation of the selectivity and temperature, the Van't Hoff equation can be used to calculate the thermodynamic parameters:

$$\ln K_{MH} = \left(\frac{\Delta S}{R}\right) - \left(\frac{\Delta H}{R}\right)\frac{1}{T}. \tag{8}$$

According to Eq. (8), ln K_{MH} versus $1/T$ plot should be straight line from which the entropy change and the enthalpy of ion-exchange process can be obtained. Fig. 2 shows such linear plots for copper, zinc, and cadmium with the thermodynamic parameters listed in Table 4. As shown by Fig. 2, the Van't Hoff equation well fits the selectivity coefficients of metal/hydrogen systems at different temperatures. The negative values of the Gibbs free energy change (ΔG) indicate that the ion-exchange process is spontaneous; the positive enthalpy (ΔH) reveals energy is absorbed as ion exchange proceeds, and the reaction is said to be endothermic resulted in the equilibrium extent of reaction increase with increasing temperature (Sandler, 1999). The entropy changes in this study are found to be positive; it means that the increased randomness appeared on the resin–solution

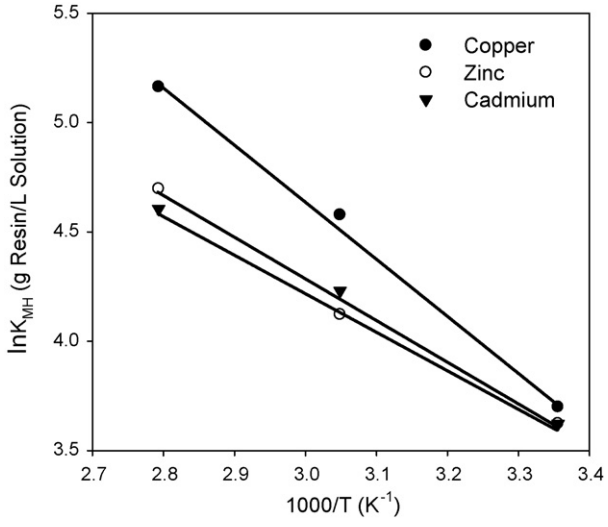

Fig. 2. The Van't Hoff plots for copper, zinc, and cadmium ion exchange on IR-120.

Table 4
Thermodynamic parameters for heavy metal ion exchange

Metal	ΔH (kJ/mol)	ΔS (J/mol K)	ΔG (kJ/mol)		
			298 K	328 K	358 K
Cu^{2+}	21.74	103.86	−9.23	−12.35	−15.46
Zn^{2+}	15.81	82.92	−8.92	−11.41	−13.89
Cd^{2+}	14.61	79.31	−9.03	−11.41	−13.79

interface during the exchange of heavy metal (Mohan *et al.*, 2002; Sekar *et al.*, 2004). The positive entropy change may be due to the release of water molecule produced by ion-exchange reaction (Jain *et al.*, 2004; Li *et al.*, 2005).

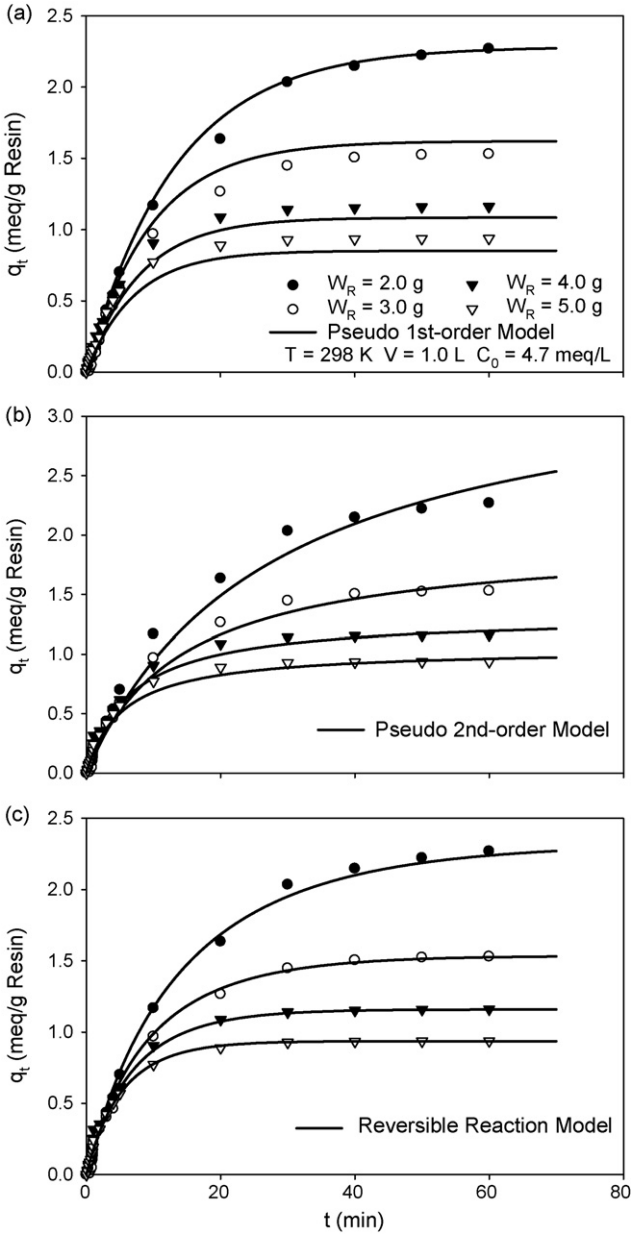

Fig. 3. Experimental and predicted copper ion-exchange curves calculated by three kinetic approaches with different resin weights at 298 K. (a) Pseudo first-order model, (b) pseudo second-order model, and (c) reversible reaction model.

3.3. Effect of resin to solution ratio on ion-exchange kinetics

The first series of experiments were performed to study the effect of the resin to solution ratio on the heavy metal ion exchange kinetics. Different amounts of resin were added to 1 L heavy metal solutions with the same initial copper concentration at 298 K. As shown by the experimental data in Fig. 3, the amounts of copper exchanged onto the resin increase rapidly at the early stage of experiment, then increase slowly, and finally approach to constant values for long experimental durations. Fig. 3 also shows that the final equilibrium copper in the resin phase decreases with increasing resin used. Because of the same amount of heavy metal present in the solution phase initially, the more resin is used to share the finite heavy metal ions, the less heavy metal per resin will be exchanged.

The kinetic curves in Fig. 3 can be described by suitable kinetic models. The first kinetic model used is the Lagergren first-order model that was also used for the analysis of

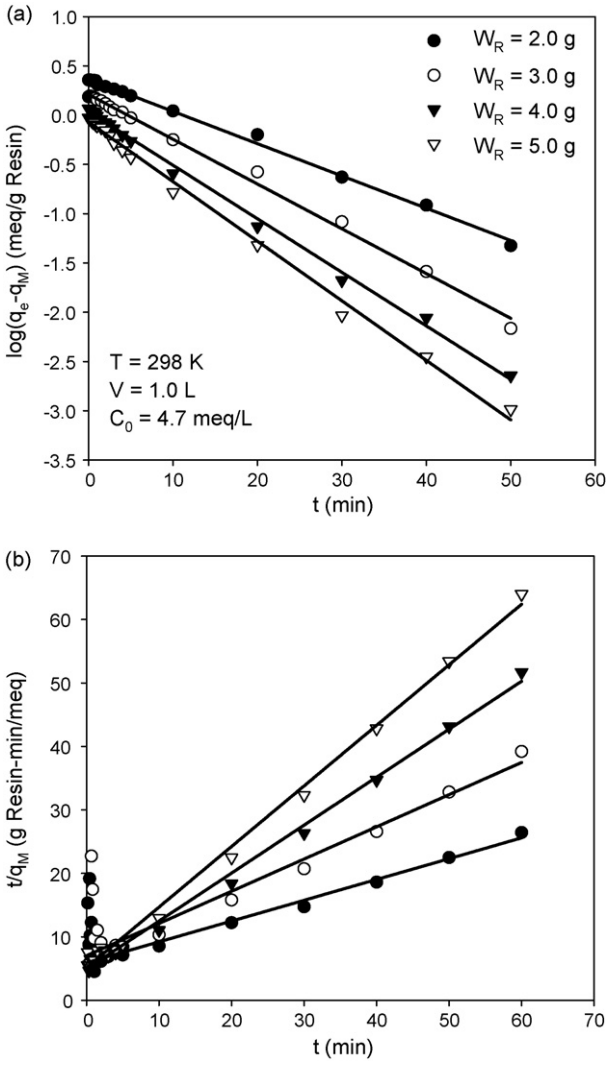

Fig. 4. Linear plots of copper ion exchange kinetics for (a) pseudo first- and (b) pseudo second-order models with different resin weights at 298 K.

Table 5
Model parameters of different ion-exchange kinetic models at 298 K

Parameter		Pseudo first-order			Pseudo second-order			Reversible
C_0	W_R	k_1	q_e	R^2	k_2	q_e	R^2	
Copper								
4.7	2.0	0.075	2.284	0.9971	0.010	3.529	0.8016	$k_a = 1.235 \times 10^{-3}$
4.7	3.0	0.105	2.319	0.9960	0.031	1.971	0.9119	$K_{MH} = 40.43$
4.7	4.0	0.125	1.621	0.9971	0.116	1.324	0.9951	$R^2 = 0.9930$
4.7	5.0	0.139	1.084	0.9955	0.179	1.048	0.9959	
2.6	2.0	0.076	1.183	0.9965	0.089	1.423	0.9926	
1.4	2.0	0.079	0.607	0.9963	0.206	0.744	0.9937	
0.5	2.0	0.095	0.237	0.9931	0.686	0.295	0.9951	
Zinc								
4.7	2.0	0.090	2.118	0.9936	0.029	2.877	0.8950	$k_a = 1.919 \times 10^{-3}$
3.3	2.0	0.094	1.442	0.9901	0.057	1.907	0.9689	$K_{MH} = 37.48$
1.8	2.0	0.094	0.789	0.9870	0.125	1.033	0.9910	$R^2 = 0.9842$
0.6	2.0	0.105	0.266	0.9856	0.459	0.348	0.9932	
Cadmium								
3.1	2.0	0.070	1.546	0.9993	0.027	2.030	0.9805	$k_a = 1.040 \times 10^{-3}$
2.3	2.0	0.080	1.149	0.9980	0.044	1.469	0.9880	$K_{MH} = 37.44$
1.5	2.0	0.093	0.765	0.9949	0.054	1.014	0.9932	$R^2 = 0.9974$
0.7	2.0	0.099	0.374	0.9973	0.232	0.442	0.9975	

adsorption kinetics (Mohan *et al.*, 2002):

$$\frac{dq_M}{dt} = k_1(q_e - q_M), \tag{9}$$

where k_1 is the rate constant of the pseudo first-order kinetic model; q_e is the metal concentration in the resin phase at equilibrium. Assuming k_1 and q_e are constant, Eq. (9) can then be integrated into a linear form with which the rate constant k_1 can be easily obtained from the slope and the intercept, respectively:

$$\log(q_e - q_M) = \log(q_e) - \left(\frac{k_1}{2.303}\right)t. \tag{10}$$

Another empirical equation, the pseudo second-order kinetic model that was also used to describe the adsorption phenomena (Lee *et al.*, 2005; Sharma and Bhattacharyya, 2005), is:

$$\frac{dq_M}{dt} = k_2(q_e - q_M)^2, \tag{11}$$

where k_2 is the rate constant of the pseudo second-order kinetic model. It can also be rewritten as the following linear form:

$$\frac{t}{q_M} = \frac{1}{k_2 q_e^2} + \left(\frac{1}{q_e}\right)t. \tag{12}$$

Similarly, the model parameters q_e and k_2 values can be calculated from the slope and intercept.

In addition to the above empirical models, we developed a reversible reaction model to describe the heavy metal ion-exchange kinetics. Although the ion-exchange kinetics is truly governed by diffusion phenomenon, the rate laws of ion-exchange reaction are quite complex and difficult to be solved. We choose a simplified but adequately acceptable approach to describe the ion-exchange kinetics. We treat the ion-exchange process as a reversible chemical reaction shown

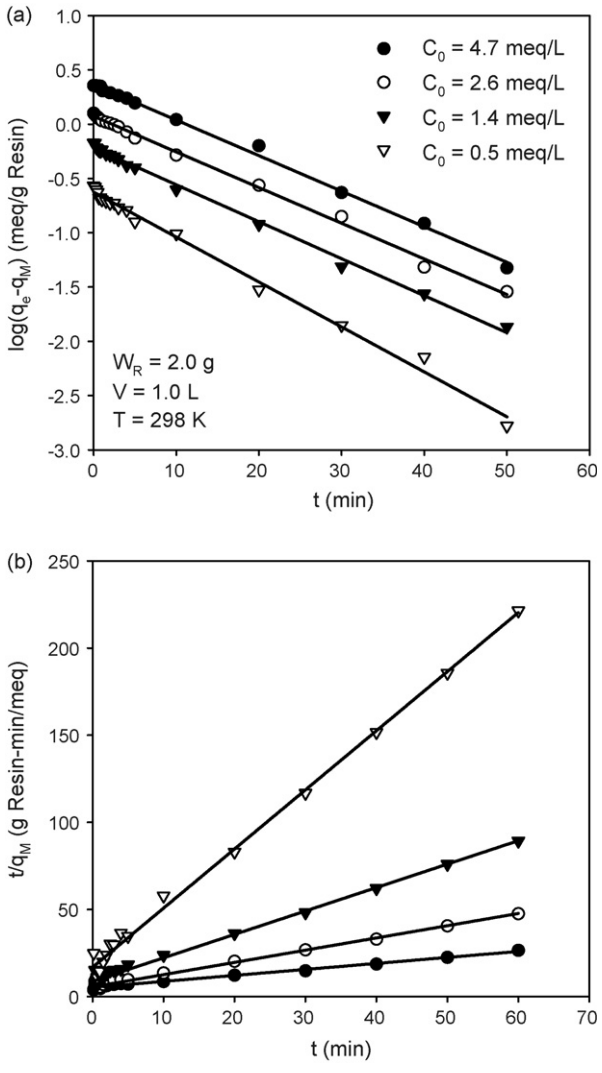

Fig. 5. Linear plots of copper ion-exchange kinetics for (a) pseudo first- and (b) pseudo second-order models with different initial metal concentrations at 298 K.

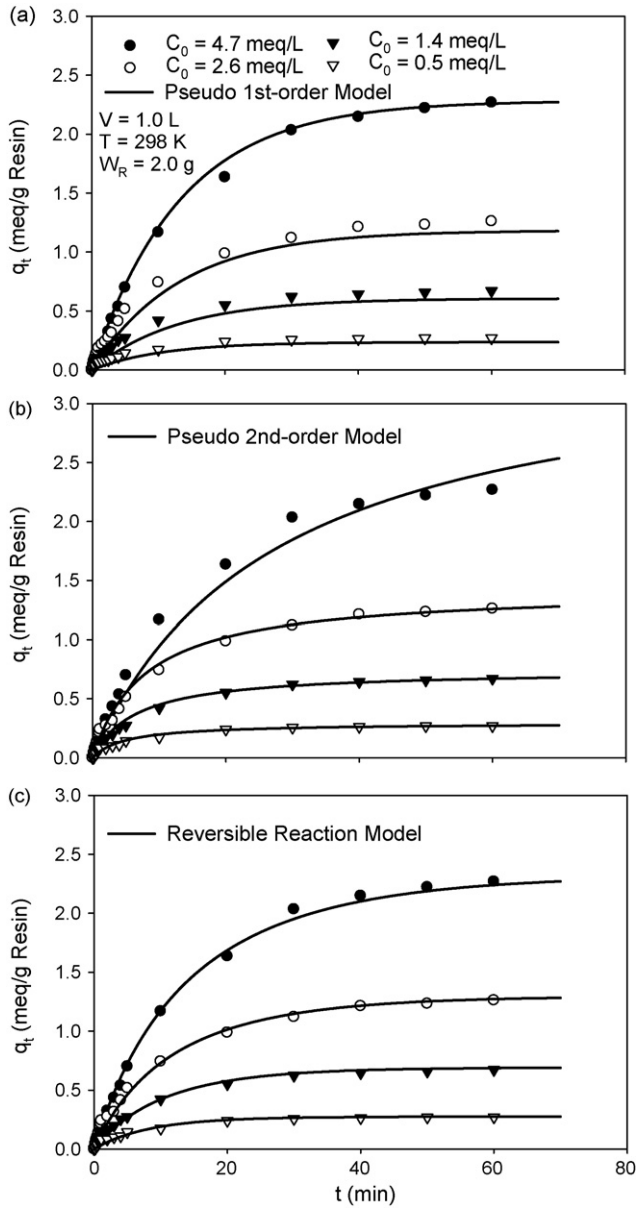

Fig. 6. Experimental and predicted copper ion-exchange curves calculated by three kinetic models with different initial metal concentrations at 298 K. (a) Pseudo first-order model, (b) pseudo second-order model, and (c) reversible reaction model.

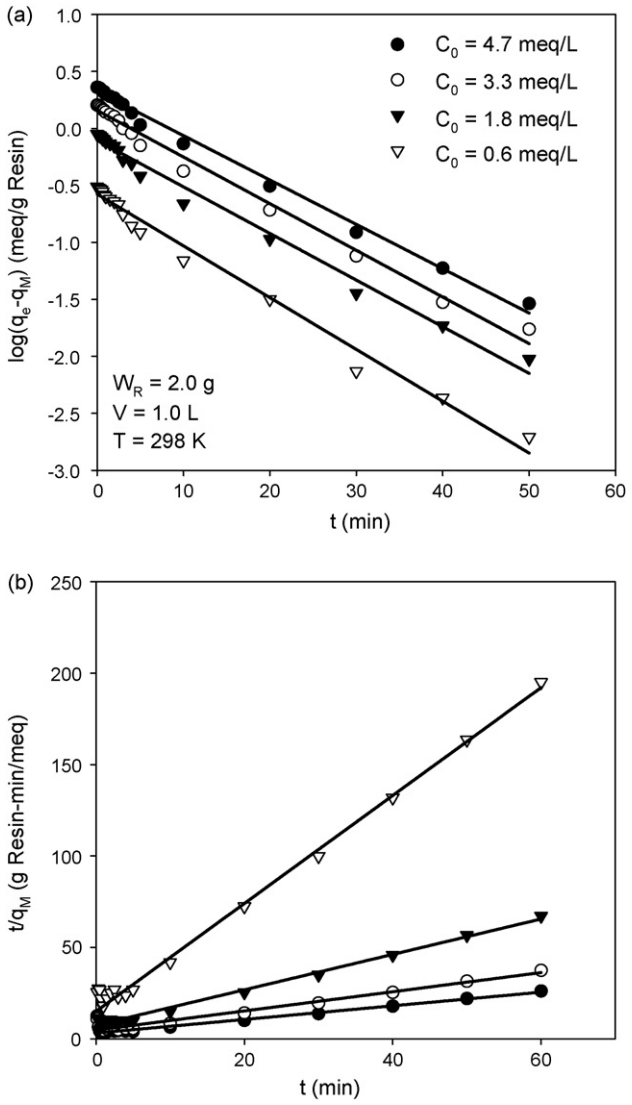

Fig. 7. Linear plots of zinc ion-exchange kinetics for (a) pseudo first- and (b) pseudo second-order models with different initial metal concentrations at 298 K.

by Eq. (13):

$$M^{2+} + 2RH \underset{k_b}{\overset{k_a}{\rightleftharpoons}} R_2M + 2H^+, \tag{13}$$

where k_a and k_b are the forward and reverse rate constants, respectively; M^{2+} is the divalent metal ions in the solution phase; RH is the ion-exchange resin in hydrogen form; R_2M is the exchanged metal onto the resin; and H^+ is the released hydrogen ion from the ion-exchange resin. The rate heavy metal removal in the solution phase can be expressed in terms of the forward and reverse rate:

$$-V \cdot \frac{dC_M}{dt} = W_R(k_a C_M q_H^2 - k_b C_H^2 q_M), \tag{14}$$

where C_M and C_H are the heavy metal and hydrogen concentrations in the solution phase, respectively; q_M and q_H are the heavy metal and hydrogen concentrations in the resin phase, respectively.

Substituting Eq. (1) into Eq. (14) leads to the following differential equation

$$-\frac{dC_M}{dt} = \left(\frac{k_a W_R}{V}\right)\left[C_M\left(q_c - \frac{V}{W_R}(C_0 - C_M)\right)^2 - \left(\frac{1}{K_{MH}}\right)(C - C_M)^2\frac{V}{W_R}(C_0 - C_M)\right], \tag{15}$$

where C_0 and C are the initial heavy metal and total cation concentrations in the solution, respectively; q_c is the total cation concentration in the resin; K_{MH} is the equilibrium constant equal to k_a/k_b. For binary ion-exchange systems, i.e., systems with two exchangeable species H^+ and M^{2+} in this study, the

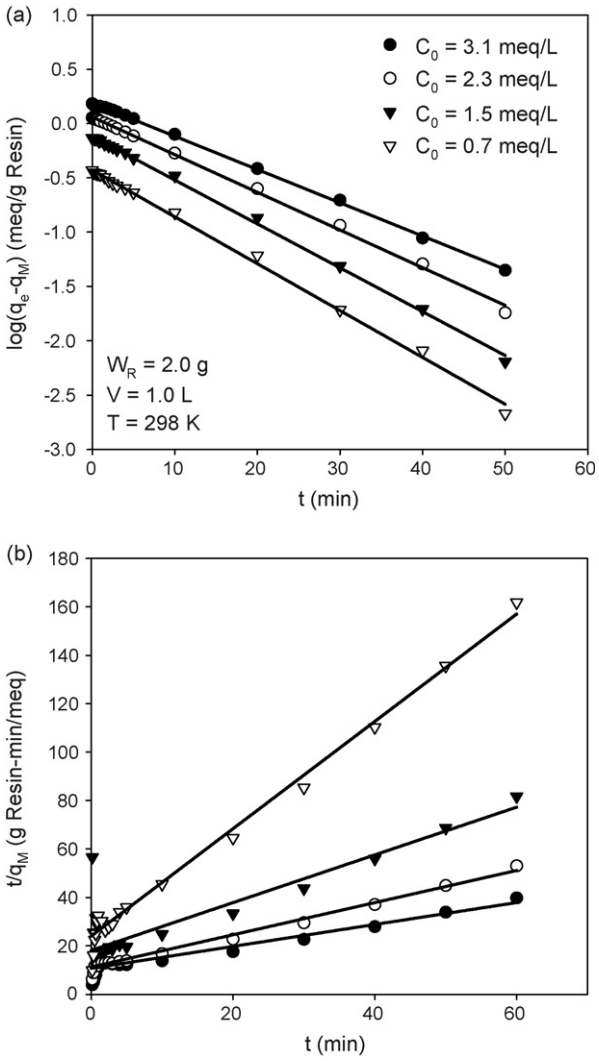

Fig. 8. Linear plots of cadmium ion exchange kinetics for (a) pseudo first- and (b) pseudo second-order models with different initial metal concentrations at 298 K.

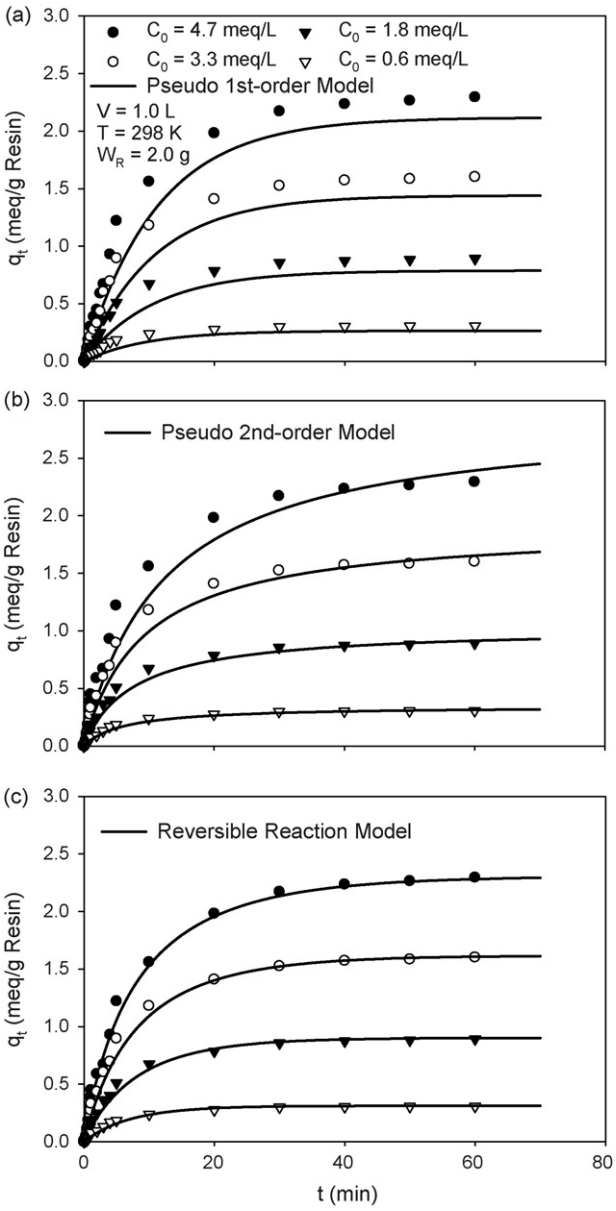

Fig. 9. Experimental and predicted zinc ion-exchange curves calculated by three kinetic models with different initial metal concentrations at 298 K. (a) Pseudo first-order model, (b) pseudo second-order model, and (c) reversible reaction model.

concentration terms can be expressed as fractions instead.

$$\begin{cases} x_M + x_H = 1 \\ y_M + y_H = 1 \end{cases} \tag{16}$$

Substituting Eq. (15) into Eq. (16) leads to a new dimensionless differential equation as shown in Eq. (17).

$$-\frac{dx_M}{dt} = \left(\frac{k_a}{F_c}\right)\left[\left(\frac{q_c}{C}\right)x_M(1-y_M)^2 - \frac{y_M}{K_{MH}}(1-x_M)^2\right], \tag{17}$$

where F_c defined in Eq. (18) is a dimensionless factor of resin capacity, resin weight, solution volume, and total solution concentration. The metal concentration in the solution phase can be calculated by multiplying metal fraction and total solution concentration $q_t = Cx_M$.

$$F_c = \frac{VC}{W_R q_c}. \tag{18}$$

The parameters were obtained from numerical methods by using DIVPAG subroutine of Compaq Visual Fortran IMSL to solve the differential equation and DBCPOL subroutine to minimize the sum of squares of the errors between the experimental and predicted copper concentrations. Once the heavy metal concentrations in the solution phase are calculated, Eq. (1) is used to calculate the heavy metal concentrations in the resin phase.

Since the pseudo first-order and second-order models are widely used in adsorption and ion-exchange processes, we use these empirical models first to fit our experimental data. Fig. 4(a) and (b) shows the linear plots of the pseudo first-order and pseudo second-order models for copper, respectively. The parameters of the pseudo first-order and pseudo second-order models are

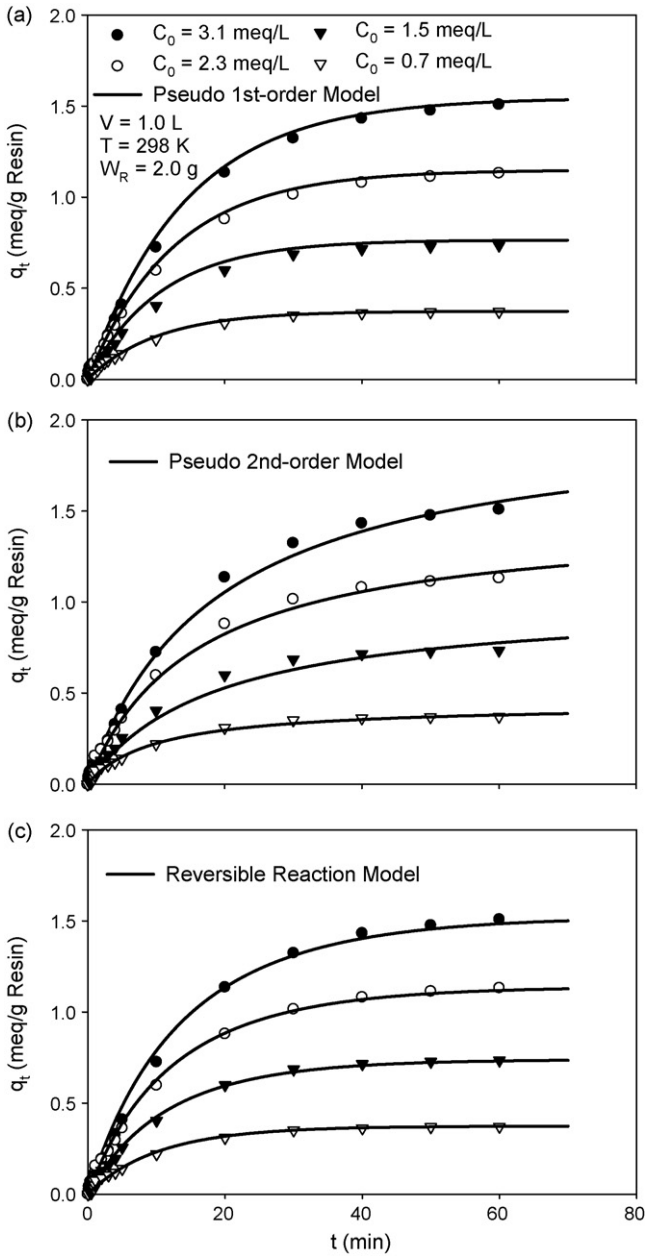

Fig. 10. Experimental and predicted cadmium ion-exchange curves calculated by three kinetic models with different initial metal concentrations at 298 K. (a) Pseudo first-order model, (b) pseudo second-order model, and (c) reversible reaction model.

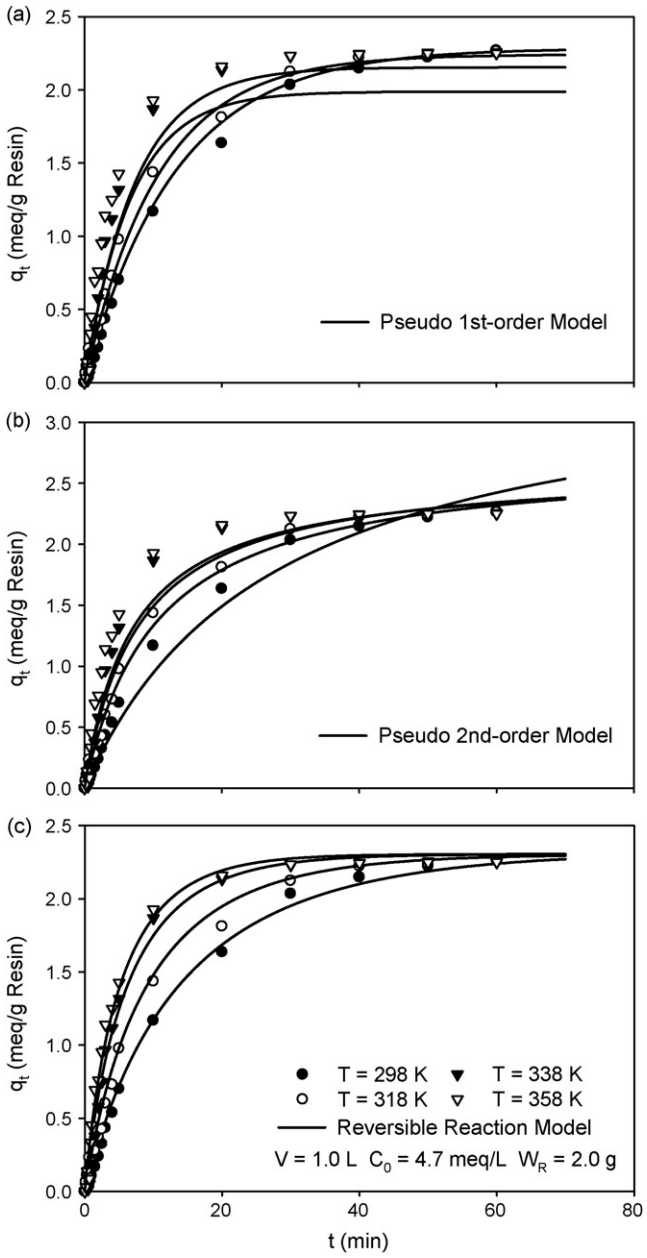

Fig. 11. Experimental and predicted copper ion-exchange curves calculated by three kinetic models at different reaction temperatures. (a) Pseudo first-order model, (b) pseudo second-order model, and (c) reversible reaction model.

summarized in Table 5. Using the model parameters the amount of copper exchanged onto the resin can be calculated and the calculated results are also shown in Fig. 3(a) and (b), respectively. Although very good linearity is found for the pseudo first-order and pseudo second-order models as shown in Fig. 4(a) and 4(b), respectively, the calculated results do not agree with the experimental data as shown by Fig. 3(a) and (b), respectively. Furthermore, the parameters k_1, k_2, and q_e vary with the amount of resin used and the initial copper concentration as shown in Table 5. Theoretically, these kinetic parameters should be independent of the reactant concentrations such as resin weight and initial heavy metal concentrations. The advantages of the pseudo first-order and pseudo second-order models are their easiness for use, but the disadvantages are the predicted results do not satisfactorily agree with the experimental data and the parameters usually depend on the operating conditions.

In order to better describe the heavy metal ion-exchange kinetics, the reversible reaction model was used to analyze the same data. In the reversible model, there is actually only one parameter k_a. All the other parameters in Eq. (17) are known a priori. The total cation concentration in the resin or the ion-exchange capacity of Amberlite IR-120 was determined by the method described by Helfferich (1962). The equilibrium constant K_{MH} can be obtained from the equilibrium study that was discussed already in the previous section. Using the model parameters listed in Table 5, the copper ion-exchange kinetic

curves can be predicted by the reversible reaction model and the results are also shown in Fig. 3(c). Comparing Fig. 3(a–c), the reversible reaction model provides a better fit to the experimental data. More important of the reversible reaction model is that the model parameters are independent of the operating conditions. Unlike the empirical models, the effect of the resin-to-solution ratio on the ion-exchange kinetics can be predicted by the reversible reaction model as shown by Eq. (17).

3.4. Effect of initial metal concentration on ion-exchange kinetics

The second series of kinetic tests were performed using different initial copper concentrations but constant amount of resin at 298 K. Similarly, very good linearity of the pseudo first-order and pseudo second-order models is obtained as shown in Fig. 5(a) and (b). But the actual fit to the experimental kinetic curves of these two models is not as satisfactory as that of the reversible reaction model, as shown in Fig. 6(a–c). The third and fourth series of kinetic tests were carried out to study the effect of initial heavy metal concentration on the zinc and cadmium ion-exchange kinetics, respectively. The experimental data are also analyzed by the three kinetic models, and the resultant model parameters are also listed in Table 5. Again, very good linearity is obtained for the pseudo first-order and pseudo second-order models, as shown in Figs. 7 and 8, for zinc and cadmium, respectively. Compared with the reversible reaction model, the two empirical models cannot give very

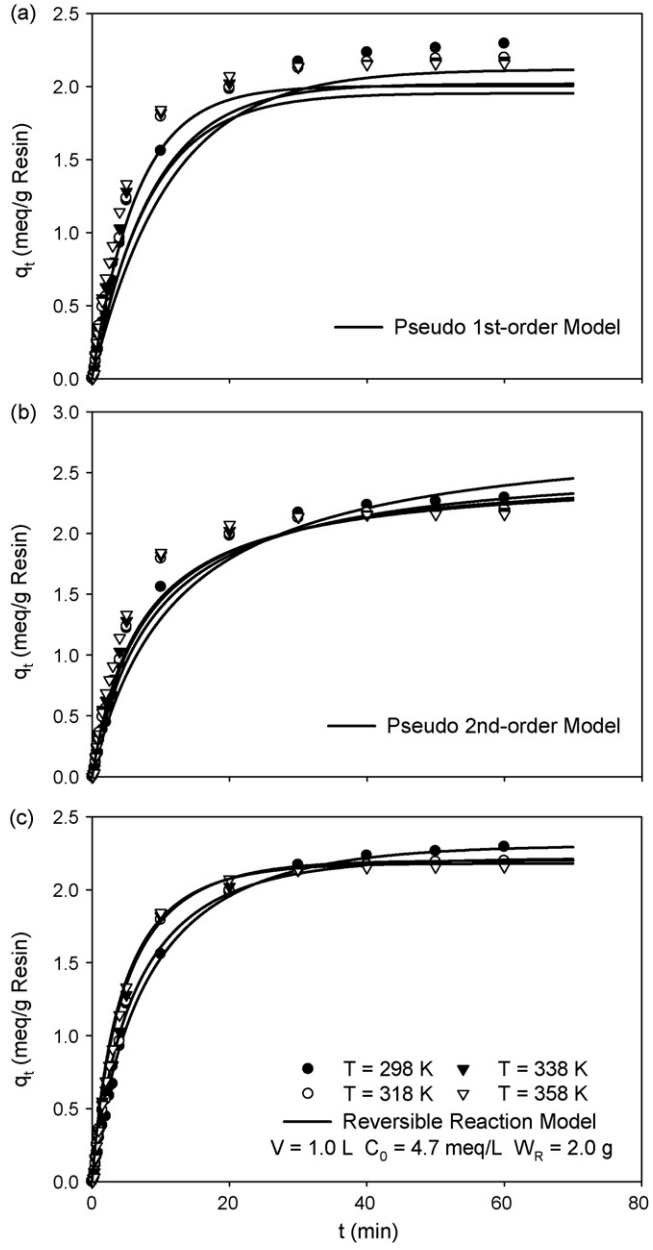

Fig. 12. Experimental and predicted zinc ion-exchange curves calculated by three kinetic models at different reaction temperatures. (a) Pseudo first-order model, (b) pseudo second-order model, and (c) reversible reaction model.

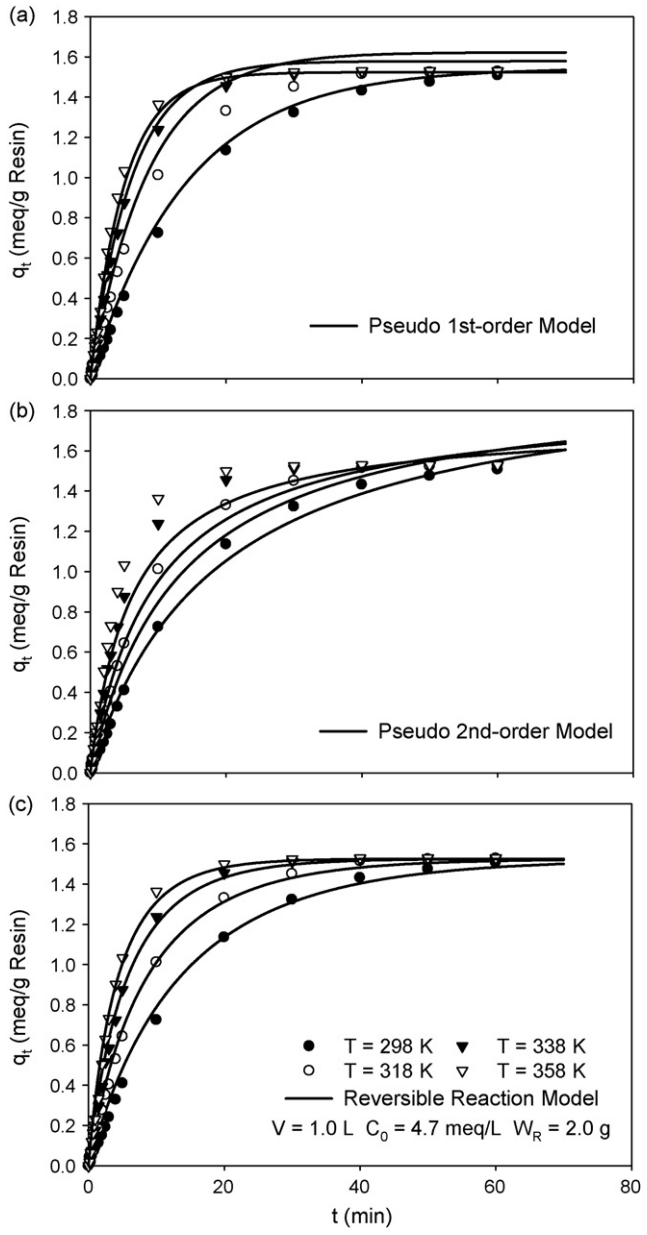

Fig. 13. Experimental and predicted cadmium ion-exchange curves calculated by three kinetic models with different reaction temperatures. (a) Pseudo first-order model, (b) pseudo second-order model, and (c) reversible reaction model.

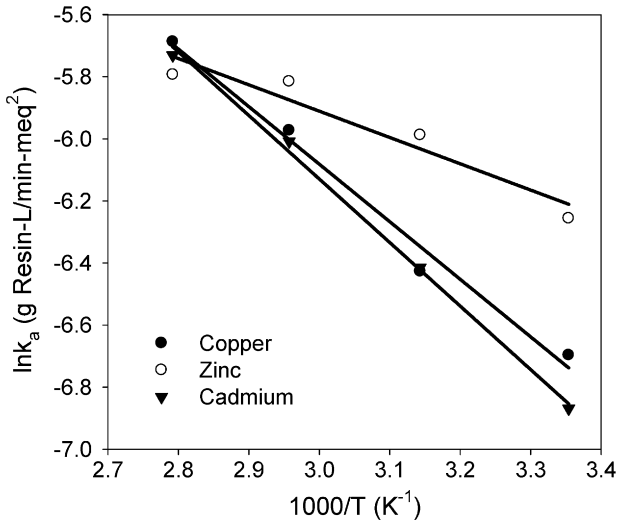

Fig. 14. The Arrhenius plots for copper, zinc, and cadmium ion exchange on IR-120.

good fit to the experimental data as shown in Figs. 9 and 10 for zinc and cadmium, respectively. Furthermore, Table 5 shows that the parameters of the two empirical models vary with the operating conditions while the parameter of the reversible reaction model for given heavy metal is independent of the operating conditions. Although not explicitly shown by Eq. (17), the amount of heavy metal exchanged onto the resin increases with increasing initial heavy metal concentration. Nevertheless, the reversible reaction model can still provide a closer fit in case of various initial metal concentrations than the pseudo first- and second-order models.

3.5. Effect of temperature on ion-exchange kinetics

The last series of kinetic tests were performed to study the effect of temperature on ion-exchange kinetics using the same resin to solution ratio and initial heavy metal concentration. The above three different kinetic models were used to fit the kinetic curves and the comparisons of the data fitting for copper, zinc, and cadmium are shown in Figs. 11–13, respectively. Table 6 summarizes the kinetic parameters of the three models. It is important to note that the selectivity coefficients K_{MH} at 318 and 338 K are calculated from the Van't Hoff equation using the thermodynamic parameters listed in Table 4. Similarly, although the high values of R^2 shown in Table 6 suggest the pseudo first-order and second-order models may be used to fit the ion-exchange kinetic data, the goodness of fitting for both empirical models is not as good as that for the reversible reaction model as shown by the comparison in Figs. 11–13.

Since the reversible reaction model gives closer prediction to the ion-exchange kinetic curves, the forward rate coefficients k_a at different temperatures are further analyzed. The Arrhenius equation is used to correlate the forward rate coefficients at different temperatures (Fogler, 1999):

$$k_a = Ae^{-E_a/RT}, \tag{19}$$

where E_a is the activation energy and A is a constant. Eq. (19) can be rewritten to a linear form from which the activation energy can be calculated from the slope:

$$\ln k_a = \ln A - \left(\frac{E_a}{R}\right)\frac{1}{T}. \tag{20}$$

Fig. 14 shows such linear plots for copper, zinc, and cadmium with the Arrhenius equation parameters listed in Table 7. As shown by the activation energy in Table 7, the

Table 7
Arrhenius parameters for heavy metal ion exchange

Heavy metal	Cu^{2+}	Zn^{2+}	Cd^{2+}
E_a (kJ/mol)	15.412	7.044	17.014
A (L/mmol min)	0.595	0.034	1.010
R^2	0.9853	0.9198	0.9971

Table 6
Model parameters of ion-exchange kinetics at different reaction temperatures

Parameter		Pseudo first-order			Pseudo second-order			Reversible		
T	C_0	k_1	q_e	R^2	k_2	q_e	R^2	$k_1 \times 1000$	K_{MH}[a]	R^2
Copper										
298	4.7	0.075	2.284	0.9971	0.010	3.529	0.8016	1.235	40.43	0.9930
318	4.6	0.093	2.241	0.9945	0.035	2.723	0.9846	1.618	71.89	0.9949
338	4.6	0.136	2.154	0.9947	0.049	2.646	0.9711	2.548	116.88	0.9916
358	4.6	0.148	1.988	0.9932	0.055	2.606	0.9508	3.389	174.82	0.9862
Zinc										
298	4.7	0.090	2.118	0.9936	0.029	2.877	0.8950	1.919	37.48	0.9842
318	4.5	0.115	2.019	0.9923	0.043	2.621	0.9112	2.510	54.50	0.9955
338	4.4	0.119	1.955	0.9911	0.053	2.534	0.9729	2.982	77.60	0.9929
358	4.5	0.153	2.005	0.9971	0.057	2.501	0.9340	3.048	109.66	0.9970
Cadmium										
298	3.1	0.070	1.546	0.9993	0.027	2.030	0.9805	1.040	37.44	0.9974
318	3.1	0.118	1.623	0.9923	0.039	1.953	0.9758	1.638	55.42	0.9984
338	3.1	0.165	1.579	0.9986	0.057	1.858	0.9572	2.459	76.83	0.9976
358	3.1	0.201	1.523	0.9978	0.094	1.746	0.9755	3.245	100.07	0.9960

[a] K_{MH} at 318 and 338 K are calculated from Eq. (8) using the thermodynamic parameters in Table 4.

energy barrier of zinc ion exchange is lower than those of copper and cadmium.

Using parameters listed in Table 7 and Eq. (19), the forward rate coefficient at a given temperature can be calculated. Similarly, using the parameters listed in Table 4 and Eq. (8), the selectivity coefficient at a given temperature can be calculated. The effect of temperature on ion-exchange kinetics can therefore be predicted by Eq. (17).

4. Conclusion

A series of ion-exchange equilibrium and kinetic tests were performed in this study, and the experimental data were interpreted by widely used approaches (Langmuir and Freundlich isotherm for equilibrium), models (pseudo first- and second-order models for kinetics), and new approach (reversible reaction model with selectivity coefficient) developed in this study. According to the results, the following conclusions can be made:

- The Langmuir isotherm fits the ion-exchange equilibrium data better than the Freundlich approach.
- The mass action law of the reversible reaction model also fits the ion-exchange equilibrium data well.
- The affinity sequence demonstrated from the selectivity coefficient is $Cu^{2+} > Zn^{2+} > Cd^{2+} > H^{+}$.
- The thermodynamic parameters of the ion-exchange process were calculated. Ion exchange equilibrium at temperatures 298, 328, and 358 K of Cu^{2+}/H^{+}, Zn^{2+}/H^{+}, and Cd^{2+}/H^{+} are found to be endothermic processes. The negative values of the Gibbs free energy change (ΔG) confirm that the ion-exchange process is spontaneous.
- The pseudo first- and second-order models, using two adjustable parameters, are easy to use to analyze the ion-exchange kinetic data. However, the associated kinetic parameters depend on the operating conditions.
- The activation energies of the ion-exchange process were calculated from the reversible reaction model parameters at different temperatures.
- Different experimental conditions of resin-to-solution ratio, initial heavy metal concentration, and temperature on the ion-exchange kinetics can be predicted more accurately by the reversible reaction model than the pseudo first- and second-order models. Only a single adjustable parameter for the reversible reaction model was used to fit the ion-exchange curves.

Acknowledgement

The financial support from National Science Council of Taiwan, Republic of China under grant NSC 93-2214-E-036-002 is highly appreciated.

References

Aksu, Z. and G. Dönmez, "Comparison of Copper(II) Biosorptive Properties of Live and Treated *Candida sp*," *J. Environ. Sci. Health*, **A36**, 367 (2001).

Bhattacharyya, K. G. and A. Sharma, "Adsorption of PB(II) from Aqueous Solution by *Azadirachta indica* (Neem) Leaf Power," *J. Hazard. Mater.*, **B113**, 97 (2004).

Chiron, N., R. Guilet, and E. Deydier, "Adsorption of Cu(II) and Pb(II) onto a Grafted Silica: Isotherms and Kinetic Models," *Water Res.*, **37**, 3079 (2003).

Choi, J. H., S. D. Kim, S. H. Noh, S. J. Oh, and W. J. Kim, "Adsorption Behaviors of Nano-Sized ETS-10 and Al-Substituted-ETAS-10 in Removing Heavy Metal Ions, Pb^{2+} and Cd^{2+}," *Micropor. Mesopor. Mater.*, **87**, 163 (2006).

Dorfner, K., *Ion Exchangers*, Walter de Gruvter Berlin, Germany (1991).

Dranoff, J. S. and L. Lapidus, "Multicomponent Ion Exchange Column Calculations," *Ind. Eng. Chem.*, **50**, 1648 (1958).

Dranoff, J. S. and L. Lapidus, "Ion Exchange in Ternary Systems," *Ind. Eng. Chem.*, **53** (1), 71 (1961).

Ersoz, M., E. Pehlivan, H. J. Duncan, S. Yildiz, and M. Pehlivan, "Ion Exchange Equilibria of Heavy Metals in Aqueous Solution on New Chelating Resins of Sporopollenin," *Reactive Polymers*, **24**, 195 (1995).

Evans, J. R., W. G. Davids, J. D. MacRae, and A. Amirbahman, "Kinetics of Cadmium Uptake by Chitosan-Based Crab Shells," *Water Res.*, **36**, 3219 (2002).

Fernández, Y., E. marañón, L. Castrillón, and I. Vázquez, "Removal of Cd and Zn from Inorganic Industrial Waste Leachate by Ion Exchange," *J. Hazard. Mater.*, **B126**, 169 (2005).

Fogler, H. S., "Elements of Chemical Reaction Engineering," 3rd Ed., Prentice-Kall International, New Jersey, U.S.A. (1999).

Helfferich, F., "Ion Exchange, McGraw-Hill, New York, U.S.A (1962).

Jain, C. K., D. C. Singhal, and M. K. Sharma, "Adsorption of Zinc on Bed Sediment of River Hindon: Adsorption Models and Kinetics," *J. Hazard. Mater.*, **B114**, 231 (2004).

Juang, R. S., H. C. Kuo, and F. Y. Liu, "Ion Exchange Recovery of Ni(II) from Simulated Electroplating Waste Solutions Containing Anionic Ligands," *J. Hazard. Mater.*, **B128**, 53 (2006).

Kapoor, A. and T. Viraraghavan, "Biosorption of Heavy Metals on *Aspergillus niger*: Effect of Pretreatment," *Bioresource Technol.*, **63**, 109 (1998).

Kiefer, R. and W. H. Höll, "Sorption of Heavy Metals onto Selective Ion-Exchange Resins with Aminophoshonate Functional Groups," *Ind. Eng. Chem. Res.*, **40**, 4570 (2001).

Kilislioglu, A. and B. Bilgin, "Thermodynamic and Kinetic Investigations of Uranium Adsorption on Amberlite IR-118H Resin," *Appl. Radiat. Isot.*, **58**, 155 (2003).

Kryvoruchko, A. P., I. D. Atamanenko, and L. Y. Yurlova, "Concentration/Purification of Co(II) Ions by Reverse Osmosis and Ultrafiltration Combined with Sorption on Clay Mineral Montmorillonite and Cation-Exchange Resin KU-2-8n," *J. Membr. Sci.*, **228**, 77 (2004).

Lee, K., Z. Wu, and H. Joo, "Kinetics and Thermodynamics of the Organic Dye Adsorption on the Mesoporous Hybrid Xerogel," *Chem. Eng. J.*, **112**, 227 (2005).

Lee, I. H., Y. C. Kuan, and J. M. Chern, "Factorial Experimental Design for Recovering Heavy Metals from Sludge with Ion-Exchange Resin," *J. Hazard. Mater.*, **B138**, 549 (2006).

Li, Y. H., Z. Di, J. Ding, D. Wu, Z. Luan, and Y. Zhu, "Adsorption Thermodynamic, Kinetic and Desorption Studies of Pb^{2+} on Carbon Nanotubes," *Water Res.*, **39**, 605 (2005).

Lin, L. C. and R. S. Juang, "Ion-Exchange Equilibria of Cu(II) and Zn(II) from Aqueous Solutions with Chelex 100 and Amberlite IRC748 Resins," *Chem. Eng. J.*, **112**, 211 (2005).

Lyubchik, S. I., A. I. Lyubchik, O. L. Galushko, L. P. Tikhonova, J. Vital, I. M. Fonseca, and S. B. Lyubchik, "Kinetics and Thermodynamics of the Cr(III) Adsorption on the Activated Carbon from Co-Mingled Wastes," *Colloids Surf. A: Physicochem. Eng. Aspects*, **242**, 151 (2004).

Mohammadi, T., A. Razmi, and M. Sadrzadeh, "Effect of Operating Parameters on Pb^{2+} Separation from Wastewater Using Electrodialysis," *Desalination*, **167**, 379 (2004).

Mohammadi, T., A. Moheb, M. Sadrzadeh, and A. Razmi, "Modeling of Metal Ion Removal from Wastewater by Electrodialysis," *Sep. Purif. Technol.*, **41**, 73 (2005).

Mohan, D., K. P. Singh, G. Singh, and K. Kumar, "Removal of Dyes from Wastewater Using Fly Ash, a Low-Cost Adsorbent," *Ind. Eng. Chem. Res.*, **41**, 3688 (2002).

Park, S. J. and Y. M. Kim, "Adsorption Behaviors of Heavy Metal Ions onto Electrochemically Oxidized Activated Carbon Fibers," *Mater. Sci. Eng.*, **A391**, 121 (2005).

Ribeiro, M. H. L. and I. A. C. Ribeiro, "Recovery of Erythromycin from Fermentation Broth by Adsorption onto Neutral and Ion-Exchange Resins," *Sep. Purif. Technol.*, **45**, 232 (2005).

Sağ, Y. and T. Kutsal, "Biosorption of Heavy Metals by Zoogloea Ramigera: Use of Adsorption Isotherms and a Comparison of Biosorption Characteristics," *Chem. Eng. J.*, **60**, 181 (1995).

Sandler, S. I., *Chemical and Engineering Thermodynamics*, 3rd Ed., John Wiley & Sons, New York, U.S.A. (1999).

Schlichter, B., V. Mavrov, T. Erwe, and H. Chmiel, "Regeneration of Bonding Agents Loaded with Heavy Metals by Electrodialysis with Bipolar Membranes," *J. Membr. Sci.*, **232**, 99 (2004).

Sekar, M., V. Sakthi, and S. Rengaraj, "Kinetics and Equilibrium Adsorption Study of Lead(II) onto Activated Carbon Prepared from Coconut Shell," *J. Colloid Interface Sci.*, **279**, 307 (2004).

Sharma, A. and K. G. Bhattacharyya, "*Azadirachta indica* (Neem) Leaf Power as a Biosorbent for Removal of Cd(II) from Aqueous Medium," *J. Hazard. Mater.*, **B125**, 102 (2005).

Suh, J. H. and D. S. Kim, "Comparison of Different Sorbents (Inorganic and Biological) for the Removal of Pb^{2+} from Aqueous Solutions," *J. Chem. Technol. Biotechnol.*, **75**, 279 (2000).

Tarley, C. R. T. and M. A. Z. Arruda, "Biosorption of Heavy Metals Using Rice Milling By-Products. Characterisation and Application for Removal of Metals from Aqueous Effluents," *Chemosphere*, **54**, 987 (2004).

Ujang, Z. and G. K. Anderson, "Performance of Low Pressure Reverse Osmosis Membrane (LPROM) for Separating Mono- and Divalent Ions," *Water Sci. Technol.*, **38**, 521 (1998).

Valverde, J. L., A. de Lucas, M. Gonzalez, and J. F. Rodriguez, "Equilibrium Data for the Exchange of Cu^{2+}, Cd^{2+}, and Zn^{2+} Ions for H^+ on the Cationic Exchanger Amberlite IR-120," *J. Chem. Eng. Data*, **47**, 613 (2002).

Yu, B., Y. Zhang, A. Shukla, S. Shukla, and K. L. Dorris, "The Removal of Heavy Metal from Aqueous Solutions by Sawdust Adsorption-Removal of Copper," *J. Hazard. Mater.*, **B80**, 33 (2000).

重金屬與離子交換樹脂之平衡暨動力學

李逸先　管郁中　陳嘉明
大同大學化學工程研究所

摘　要

離子交換樹脂對於去除工業廢水或污泥中之重金屬，皆有其潛力，欲設計及操作重金屬之去除程序，須先知道重金屬離子與離子交換樹脂間之平衡暨動力學關係。本研究首先以批式實驗之方法，測量 Cu^{2+}/H^+、Zn^{2+}/H^+及 Cd^{2+}/H^+系統於強酸型陽離子交換樹脂 IR-120 之離子交換平衡關係。以 Langmuir、Freundlich 及選擇係數等平衡模式對液相與固相中之重金屬濃度進行非線性回歸，並針對不同溫度下之結果進行熱力學探討。結果顯示，比較選擇係數大小所得之親和力序列為 $Cu^{2+} > Zn^{2+} > Cd^{2+} > H^+$。而離子交換動力學之實驗結果以擬一階、擬二階及可逆反應模式進行理論分析，根據所得之反應速率常數計算之活化能分別為銅 15.41 kJ/mol、鋅 7.04 kJ/mol、鎘 17.01 kJ/mol。雖然擬一階及擬二階模式可簡易並快速地分析實驗結果，但回歸參數卻會因實驗條件之不同而有所變化。因此，本研究選擇以可逆反應模式探討不同樹脂重量、起始重金屬濃度及反應溫度對離子交換動力學之影響。